

Glacial-interglacial sea surface temperature changes across the subtropical front east of New Zealand based on alkenone unsaturation ratios and foraminiferal assemblages

E. L. Sikes¹ and W. R. Howard

Cooperative Research Centre for Antarctic and Southern Ocean Environment, Hobart, Tasmania, Australia

H. L. Neil

National Institute for Water and Atmosphere, Kilbirnie, Wellington, New Zealand

J. K. Volkman²

CSIRO Marine Research, Hobart, Tasmania, Australia

Received 12 March 2001; revised 22 January 2002; accepted 22 January 2002; published 30 April 2002.

[1] We present sea surface temperature (SST) estimates based on the relative abundances of long-chain C_{37} alkenones ($U_{37}^{K'}$) in four sediment cores from a transect spanning the subtropical to subantarctic waters across the subtropical front east of New Zealand. SST estimates from $U_{37}^{K'}$ are compared to those derived from foraminiferal assemblages (using the modern analog technique) in two of these cores. Reconstructions of SST in core tops and Holocene sediments agree well with modern average summer temperatures of $\sim 18^{\circ}\text{C}$ in subtropical waters and $\sim 14^{\circ}\text{C}$ in subpolar waters, with a $4^{\circ}\text{--}5^{\circ}\text{C}$ gradient across the front. Down core $U_{37}^{K'}$ SST estimates indicate that the regional summer SST was $4^{\circ}\text{--}5^{\circ}\text{C}$ cooler during the last glaciation with an SST of $\sim 10^{\circ}\text{C}$ in subpolar waters and an SST of $\sim 14^{\circ}\text{C}$ in subtropical waters. Temperature reconstructions from foraminiferal assemblages agree with those derived from alkenones for the Holocene. In subtropical waters, reconstructions also agree with a glacial cooling of 4° to $\sim 14^{\circ}\text{C}$. In contrast, reconstructions for subantarctic pre-Holocene waters indicate a cooling of 8°C with glacial age warm season water temperatures of $\sim 6^{\circ}\text{C}$. Thus the alkenones suggest the glacial temperature gradient across the front was the same or reduced slightly to $3.5^{\circ}\text{--}4^{\circ}\text{C}$, whereas foraminiferal reconstructions suggest it doubled to 8°C . Our results support previous work indicating that the STF remained fixed over the Chatham Rise during the Last Glacial Maximum. However, the differing results from the two techniques require additional explanation. A change in euphotic zone temperature profiles, seasonality of growth, or preferred growth depth must have affected the temperatures recorded by these biologically based proxies. Regardless of the specific reason, a differential response to the environmental changes between the two climate regimes by the organisms on which the estimates are based suggests increased upwelling associated with increased winds and/or a shallowing of the thermocline associated with increased stratification of the surface layer in the last glaciation. *INDEX TERMS:* 4267 Oceanography: General: Paleoceanography; 4850 Oceanography: Biological and Chemical: Organic marine chemistry; 1050 Geochemistry: Marine geochemistry (4835, 4850); 1055 Geochemistry: Organic geochemistry; *KEYWORDS:* paleoceanography, sea surface temperature, alkenones, Southern Ocean, Last Glacial Maximum

1. Introduction

[2] Surface conditions in the Southern Ocean influence intermediate and deep water formation. Today, subpolar to subtropical thermal gradients in the Southern Ocean vary seasonally with the annual climate cycle. Accompanying the glacial to interglacial climate change, the temperature gradients are thought to have migrated by a few degrees of latitude [Howard and Prell, 1992] which would have affected both surface water circulation and regional climate systems. In order to clarify the Southern Ocean's influence on global climate it is essential

to determine the variations in sea surface temperature (SST) and frontal locations between the Holocene and the Last Glacial Maximum.

[3] The subtropical front (STF, also known as the subtropical convergence, or STC), considered to be the northern extent of the Southern Ocean, is the frontal zone marking the boundary between the subtropical gyre and subantarctic waters. The STF is defined by the distinct temperature, salinity, and nutrient gradients between the two converging water masses. The subtropical surface waters to the north of the STF are oligotrophic, warm, and saltier (~ 35.8 practical salinity units (psu) in this location) flowing south in the East Cape Current from the South Pacific gyre to the Chatham Rise. Subantarctic waters are nutrient-rich, and salinities are lower (~ 34.5 psu) than in subtropical waters [Butler *et al.*, 1992]. Hydrographically, the subtropical front is best defined by salinity (the 34.81 psu halocline in this area) [Edwards and Emery, 1982] or the 11°C isotherm at ~ 100 m depth, which does not vary with season [Belkin and Gordon, 1996; Rintoul *et al.*, 1997]. However, for paleoceanographic reconstructions the front is more usefully identified by a surface

¹Now at Institute of Marine and Coastal Sciences, Rutgers, State University of New Jersey, New Brunswick, New Jersey, USA.

²Also at Cooperative Research Centre for Antarctic and Southern Ocean Environment, Hobart, Tasmania, Australia.

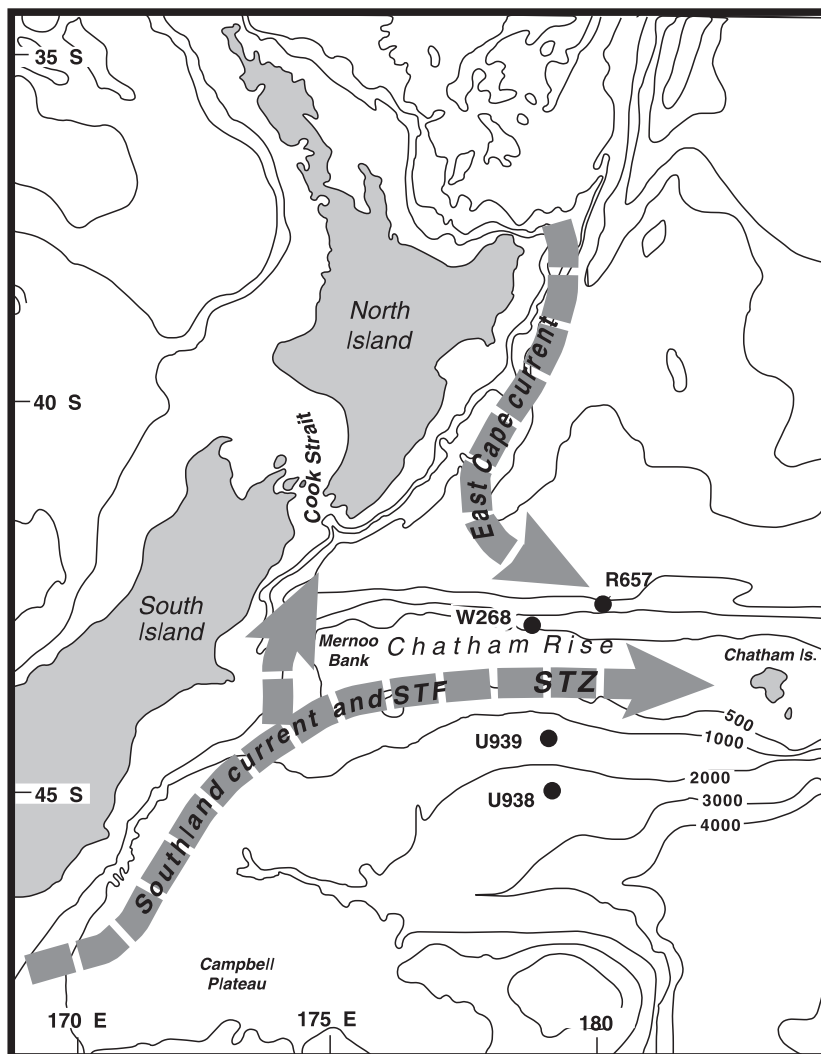


Figure 1. Map of the study area. The subtropical front runs across the bathymetric high of the Chatham Rise and marks the boundary between subtropical waters to the north and subpolar (Southern Ocean) waters to the south. The circles mark the location of the cores used in this study; Table 1 gives their locations and depths.

temperature change (or gradient) of $\sim 4^{\circ}\text{C}$ across $\sim 1^{\circ}$ latitude. Temperatures at the STF vary seasonally and zonally across the Southern Ocean. East of New Zealand the temperature difference south to north across the front is generally $10^{\circ}\text{--}14^{\circ}\text{C}$ in the winter and $14^{\circ}\text{--}18^{\circ}\text{C}$ in the summer [cf. *Belkin and Gordon, 1996; Chiswell, 1994*].

[4] The core of the modern STF is located at $\sim 45^{\circ}\text{S}$ in the Tasman Sea [*Belkin and Gordon, 1996; Edwards and Emery, 1982; Rintoul et al., 1997*]. East of New Zealand the STF runs north along the South Island as the Southland current until it turns east again, astride the Chatham Rise, $1^{\circ}\text{--}3^{\circ}$ farther north than its position in the south Tasman Sea [*Belkin and Gordon, 1996; Edwards and Emery, 1982; Rintoul et al., 1997*]. The rise is a 1000 km long submerged continental plateau, with water depths over the rise of 400 m extending east of New Zealand at 44°S (Figure 1). With depths in areas as shallow as 200 m, the STF is believed to be bathymetrically locked at the rise [*Heath, 1981, 1985*]. Nonetheless, its exact location varies continually north-south across the rise on mesoscale time frames [*Belkin and Gordon, 1996; Chiswell, 1994; Uddstrom and Oien, 1999*] as it does elsewhere in the Southern Ocean [*Belkin and Gordon, 1996*].

East of the Chatham Rise, at locations free from bathymetric constraints, it moves south again to $\sim 47^{\circ}\text{S}$ [*Heath, 1981*].

[5] During the last glaciation the STF shifted $3^{\circ}\text{--}5^{\circ}$ farther north from its present location in the Indian Ocean [*Bé and Duplessy, 1976; Morley, 1989; Prell et al., 1979; Howard, 1992*] and to the south of Australia [*Wells and Okada, 1996; Wells and Connell, 1997*]. However, east of New Zealand, studies of microfossil assemblages and SST estimates indicate that the front did not move off the rise [*Fenner et al., 1992; Weaver et al., 1998*] and remained north of 46°S in the glaciation [*Nelson et al., 1993*]. Foraminiferal transfer function sea surface temperatures (SST) reconstructions suggest that the temperature gradient across the front doubled (to 8°C) because of a greater cooling of the subpolar water mass [*Weaver et al., 1998*]. These results are supported by a reassessment of these reconstructions using other temperature conversion programs [*Barrows et al., 2000*]. However, strong cooling in subpolar waters east of New Zealand is not supported by studies of nannofossil assemblages [*Wells and Okada, 1997*]. There is evidence that subpolar waters may have leaked across the rise through the Mernoo Gap (Figure 1), causing as much as 6°C cooling of subtropical waters, but this would have

Table 1. Locations and Depths for Cores Used in This Study

Core	Side of Rise	Location		Depth, m	Length, m	Tephra, Depth, cm
		Latitude	Longitude			
R657	north	42°32'S	179°29'55"E	1408	3.03	none seen
W268	north	42°51'03"S	178°58'16"E	980	0.71	22–24
U938	south	45°04.5'S	179°30'E	2700	4.1	127–131
U939	south	44°32'S	179°30'E	1300	3.39	76–83

reduced the temperature gradient across the front, and the effect was apparently restricted to coastal waters [Fenner *et al.*, 1992; Nelson *et al.*, 2000].

[6] In this study we test these results by a direct examination of the gradient of SST across the front. We use a transect of four cores from north and south of the STF that have $<1^\circ$ latitudinal spacing on the northern and southern flanks of the Chatham Rise (north and south of the present-day STF; Figure 1 and Table 1) and compare SST estimations from two techniques, alkenone unsaturation ratios (U_{37}^K) and the modern analog technique (MAT) applied to foraminiferal assemblages. U_{37}^K has been well calibrated in Southern Ocean waters [Sikes and Volkman, 1993; Sikes *et al.*, 1997]. U_{37}^K estimates in four cores are compared to MAT estimates from two of those cores (U938 and R657) [Neil, 1997], which are the same cores used by Weaver *et al.* [1998]. By comparing SST estimates we can clarify the possible influence of surface water parameters besides temperature on these techniques. Previous work suggests that SST proxies can respond to factors other than surface temperature, such as subsurface temperatures (that might not covary with surface temperatures) or the seasonality of growth of the organisms

on which the estimates are based [Chapman *et al.*, 1996; Sikes and Keigwin, 1994, 1996; Volkman, 2000].

2. Materials and Methods

2.1. Alkenones and U_{37}^K

[7] Sediment cores were split and sampled on board ship within 24 hours of the core being retrieved and samples used for alkenone analyses were frozen immediately to -20°C in solvent-rinsed glass jars and kept frozen until extraction. Approximately 10 g of thawed wet sediment was extracted ultrasonically in chloroform and methanol to provide a total lipid extract following procedures described by Sikes *et al.* [1997]. The extracts were then saponified in 5% KOH in methanol, and the neutral fraction, containing the alkenones and alkenes, was obtained by partitioning into hexane-chloroform to remove the coeluting C_{37} triunsaturated fatty acid methyl ester and thus improve quantification [Sikes and Volkman, 1993; Sikes *et al.*, 1997]. For this study an alkenone-bearing extract from a laboratory culture of a noncalcifying haptophyte (*Isochrysis* sp. clone "T. Iso") grown at 16°C , with approximately equal

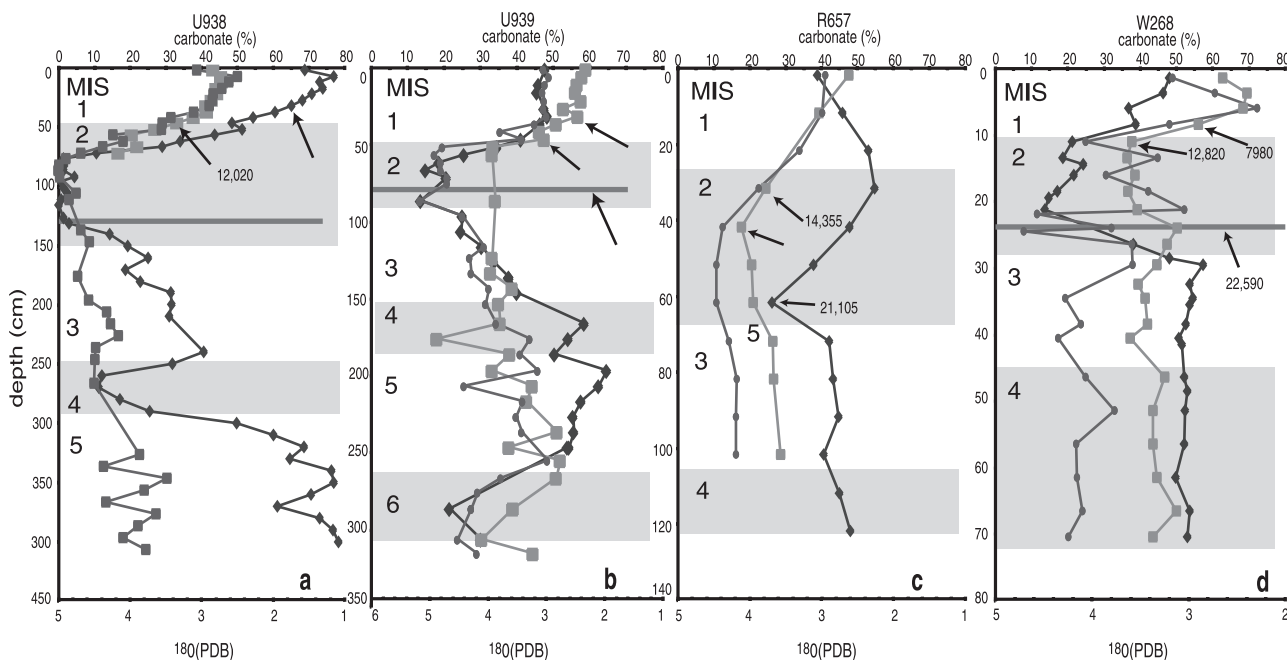


Figure 2. Stratigraphic control in study cores: (a) core U938, (b) core U939, (c) core R657, and (d) W268 core. Shading indicates placement of marine isotope stage (MIS) boundaries. Stratigraphy in the cores is based on a combination of CaCO_3 (solid diamonds), $\delta^{18}\text{O}$ on the benthic foraminifera *Uvigerina* sp. (circles) and mixed *Cibicidoides* (solid squares), the depth of the Kawakawa tephra layer in the core (horizontal shaded line, radiocarbon dated as 22,590 ^{14}C years B.P.), and radiocarbon dates (Table 2, indicated by arrows). Radiocarbon ages indicated in Figures 2a–2d are those used for stratigraphy; not all radiocarbon ages performed were considered reliable (see discussion in the text). Dates reported for some levels in R657 and U939 are averages of two ages performed on the same level (Table 2). Below the Kawakawa tephra, isotope stage 3–5 boundaries were chosen from the best fit of CaCO_3 and $\delta^{18}\text{O}$ to the curve of Martinson *et al.* [1987].

amounts of the $C_{37:2}$ and $C_{37:3}$ alkenones, $U_{37}^K = 0.521$), was used routinely as a working standard to check the analytical data. Variation in analyses of this standard over a year showed a standard deviation of $0.006 U_{37}^K$ units, which gives an analytical accuracy of approximately $\pm 0.18^\circ\text{C}$ [Sikes et al., 1997].

[8] The neutral lipid fraction was analyzed by capillary gas chromatography (GC) using a Hewlett Packard HP-1 methyl silicone fused silica column (50 m \times 0.32 mm inner diameter). The samples were injected in chloroform using a cooled OCI-3 on-column injector. Hydrogen was the carrier gas. A temperature program of $50^\circ\text{--}150^\circ\text{C}$ at $30^\circ\text{C min}^{-1}$ and $150^\circ\text{--}325^\circ\text{C}$ at 3°C min^{-1} gave good separation of all major constituents [Sikes and Volkman, 1993]. Compounds were detected with a flame ionization detector, and peak areas were measured using DAPA[™] acquisition and processing software. For final compound identification, samples were analyzed by gas chromatography mass spectrometry (GC-MS) on a Hewlett Packard 5790 MSD connected by a direct capillary inlet to a HP 5890 gas chromatograph operated as described above. Typical MSD conditions were electron energy 2200 volts, transfer line 310°C , electron energy 70 eV, 1.1 scans s^{-1} , and mass range 40–600 Da. U_{37}^K values were calculated from peak areas on the gas chromatograms and converted to temperature estimates using both the U_{37}^K calibration of Sikes and Volkman [1993] and Prahl et al. [1988].

2.2. Choice of the U_{37}^K Calibration

[9] On the Chatham Rise the Sikes and Volkman [1993] calibration based on Southern Ocean core tops provides Holocene temperature estimates in these cores that are equivalent to modern warm season (spring-summer) values. Globally, the Prahl et al. [1988] calibration ($U_{37}^K = 0.034T + 0.039$) is now considered the standard in the field, but it is not recommended for use where the calibration is environmentally unrealistic [Prahl et al., 2000]. The Prahl et al. [1988] calibration is not appropriate here for two reasons. First, the Prahl et al. [1988] regression has generally been correlated with annual average temperatures [Müller et al., 1998], but in our study we required a seasonal calibration in order to compare results directly with foraminiferal reconstructions which provide warm and cold season determinations rather than an annual average. Second, in Chatham Rise sediments the Prahl et al. [1988] calibration produces Holocene (core top) temperatures for the waters south of the STF that are equivalent to late winter temperatures, $2^\circ\text{--}4^\circ\text{C}$ colder than annual averages and $\sim 4^\circ\text{C}$ colder than spring-summer temperatures in most cores. Numerous studies suggest that the main season of growth and flux to the sediments in the waters bathing the Chatham Rise is spring and summer. In situ water column studies [Bradford-Grieve et al., 1999], sediment trap data [Nodder and Northcote, 2001], and satellite chlorophyll data [Comiso et al., 1993] all indicate that spring-summer fluxes and productivity are significantly elevated over winter levels in this area. Significantly, although blooms begin and sometimes peak in spring on the Chatham Rise [Nodder and Northcote, 2001], these blooms often persist into summer (January to March) [Comiso et al., 1993; Nodder and Northcote, 2001]. There is no evidence for productivity peaks in midwinter [Bradford-Grieve et al., 1999; Comiso et al., 1993; Nodder and Northcote, 2001]. Accordingly, we have used the Sikes and Volkman [1993] calibration ($U_{37}^K = 0.0414T - 0.156$) to calculate spring-summer SSTs in our study.

2.3. Temperature Estimates From Foraminiferal Assemblages

[10] Sediment samples used for foraminiferal assemblage and $\delta^{18}\text{O}$ analyses, after washing and drying, were sieved to $\geq 150 \mu\text{m}$ and successively split until 300–500 whole planktonic foraminifera were obtained. For faunal analyses, the 29 species and

morphotypes recognized by Kipp [1976] and used by *Climate: Long-Range Investigation, Mapping, and Prediction (CLIMAP)* [1976, 1981] were counted with two exceptions. *Globorotalia crassaformis* was excluded because of its regional disappearance from subantarctic waters $\sim 300,000$ years ago [Howard and Prell, 1992; Williams, 1976], and *Neoglobobulimina pachyderma* (dextral)-*N. dutertrei* intergrade is no longer counted as a separate taxon [Prell et al., 1999]. SST estimates were then obtained using the modern analog technique [Anderson et al., 1989; Howard and Prell, 1992; Overpeck et al., 1985; Prell, 1985].

[11] The modern analog technique matches a down core assemblage with modern core top samples that have similar faunas [Prell, 1985]. The 10 best fit core tops are chosen using squared chord distance, and the weighted (using a corresponding squared chord similarity) average of their associated temperatures is the temperature estimate. In this study the modern SST climatology is the “GOSTA” data set [Bottomley et al., 1990]. The method permits a sample by sample estimate of the fit between down core samples and modern core tops. Ancient samples with close modern analogs have low dissimilarity coefficients. This comprises one measure of the reliability of the estimate. Dissimilarity coefficients (squared chord distance) of zero are considered a perfect match, whereas a value of 2 is considered completely dissimilar. For this study, the dissimilarity coefficients are excellent; all values are < 0.2 , which are considered acceptable matches [Anderson et al., 1989]. The modern SST database used is the same as that used by CLIMAP except for the exclusion of *G. crassaformis* and *N. pachyderma* (dextral)-*N. dutertrei* intergrade in the assemblage counts [Prell et al., 1999]. Compared with CLIMAP estimates, analog estimates yield correlations equal or better to observed SST and have lower standard errors [Prell, 1985]. Assemblage counts for cores R657 and U938 were first reported by Neil [1997]. Modern analogs were rerun on these counts for this study.

2.4. Stable Oxygen Isotopes

[12] Isotope analyses were conducted following the laboratory procedures described by Neil [1997]. Approximately 5–10 individuals of mixed *Cibicidoides* species were picked from the $\geq 150 \mu\text{m}$ size fraction. Most of the samples were analyzed at the Australian National University (ANU) on a Finnigan mass spectrometer fitted with an individual bath-type automated carbonate line (a “Kiel device”). The remainder (including multiple duplicates of samples analyzed at ANU) were measured on a VG-Micromass 602D at the University of Waikato, New Zealand. All results are reported as per mil (‰) deviations from the Pee Dee belemnite (PDB) standard using the National Bureau of Standards’ NBS-20 as a laboratory standard. Analytical precision is better than 0.10‰ ($\pm 1\sigma$) based on NBS-20 replicates.

2.5. Calcium Carbonate Content

[13] Calcium carbonate contents were measured on the same subsamples used for stable isotopes and faunal studies. CaCO_3 was measured using a differential pressure technique based on that of Jones and Kateiris [1983] using the carbonate line at the National Institute for Water and Atmospheric Research (NIWA), Wellington, New Zealand [Neil, 1997]. The sampling interval was 5 cm above the Kawakawa tephra and 10 cm below the tephra (see section 3.1 for discussion). All cores in this study are now archived in the core facility at NIWA Wellington.

3. Results

3.1. Stratigraphy

[14] Estimates of ages down core are based on a combination of $\delta^{18}\text{O}$, percent carbonate, bulk ^{14}C dates, ^{14}C AMS dates,

Table 2. Radiocarbon Ages Used for Stratigraphy^a

Core	Depth, cm	Age, years B.P.	Error	Sample Number	Sample Type	Comments
R657	30–31	14,760	50	CAMS 50990	AMS, <i>G. inflata</i>	
R657	30–32	14,160	200	Wk 3771	bulk C	
R657	40–42	17,980	480	Wk 3772	bulk C	
R657	60–61	20,190	80	CAMS 50991	AMS, <i>G. inflata</i>	
R657	60–61	20,230	100	CAMS 51001	AMS, <i>G. inflata</i>	
W268	6.5–8.5	7,980	180	Wk 3756	bulk C	
W268	9.0–11.0	12,820	330	Wk 3757	bulk C	
W268	9.5–11.5	18,700	90	CAMS 50992	AMS, <i>G. inflata</i>	
W268	9.5–11.5	17,260	190	CAMS 52008	AMS, <i>G. inflata</i>	0.12 mg carbon
W268	19.5–22	12,070	50	CAMS 50993	AMS, <i>G. inflata</i>	0.21 mg carbon
W268	19.5–22	10,410	90	CAMS 52009	AMS, <i>G. inflata</i>	
W268	25–27	>40,300	NA	CAMS 50994	AMS, <i>N. pachyderma</i>	0.17mg carbon
U938	29–31	9,350	160	Wk 3767	bulk C	
U938	49–51	12,370	2110	Wk 3768	bulk C	
U938	51–53	12,000	50	CAMS 50995	AMS, <i>G. inflata</i>	avg age 12130
U938	51–53	12,030	50	CAMS 51002	AMS, <i>G. inflata</i>	
U938	69–71	17,580	580	Wk 3769	bulk C	
U939	32–34	9,830	250	Wk 3763	bulk C	
U939	40–42	13,060	50	CAMS 50999	AMS, <i>G. inflata</i>	
U939	42–44	12,630	330	Wk 3764	bulk C	
U939	50–52	14,440	70	CAMS 51000	AMS, <i>G. inflata</i>	
U939	52–54	17,710	660	Wk 3765	bulk C	
U939	62–64	23,020	1980	Wk 3766	bulk C	

^aBulk radio carbon dates were performed at the University of Waikato radiocarbon laboratories (Wk sample numbers). AMS dates were performed on monospecific samples of the planktonic foraminifera *Globorotalia inflata* or, in one case, *Neogloboquadrina pachyderma*. Suboptimal weights are noted. All AMS analyses were performed at Lawrence Livermore Laboratory (CAMS sample numbers). Ages for depths 30–32 cm and 60–61 cm in core R657 and depths 51–53 cm in core U939 were averaged in developing the depth to age conversions in those cores.

and the depth of the Kawakawa tephra in the core (Figure 2 and Table 2). The Kawakawa tephra is an excellent stratigraphic marker in this area. Its distribution in marine sediments, composition, and ¹⁴C age (22,590 ± 230 ¹⁴C years B.P.) are well established [Carter et al., 1995; Froggatt and Lowe, 1990]. The Kawakawa tephra was

identified in three cores as a distinct pink band of 2–6 cm thickness. It is absent in core R657, similar to other cores from the Hikurangi Plateau to the north of the Chatham Rise [Carter et al., 1995]. All cores in this study come from the pelagic drupe area surrounding the Chatham Rise where hemipelagic sedimentation has been continu-

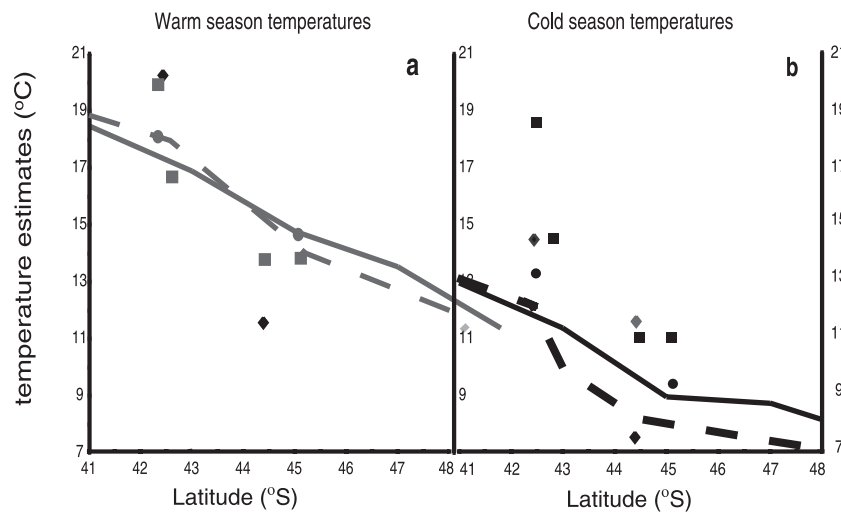


Figure 3. Comparison of core top temperature reconstructions and modern observational data for SST across the Chatham Rise. (a) Summer temperatures. Solid line shows COADS summer (February) SST. Dotted line shows satellite summer (February) SST. Squares are summer alkenone SST estimate (calculated using Sikes and Volkman [1993] calibration). Circles are summer SST modern analog technique (MAT) core tops. Diamonds are trap-based MAT summer SST reconstruction. (b) Winter temperatures. Solid line shows winter (August) COADS SST. Dotted line shows satellite winter (August) SST. Squares are subsurface alkenone SST estimates (calculated using Prahl et al. [1988] calibration). Circles are winter MAT core top SST reconstructions. Diamonds are trap-based MAT winter SST reconstruction. Summer season reconstructions (symbols in Figure 3a) fall within 2°C of the summer observational data (lines in Figure 3a), with the exception of summer trap-based MAT estimates, which are closer to winter observational data (lines in Figure 3b). Subsurface and winter SST estimates fall closer to winter observational data (Figure 3b) with the exception of alkenone-based estimates for subtropical waters, which suggests a stronger summer bias in that data set.

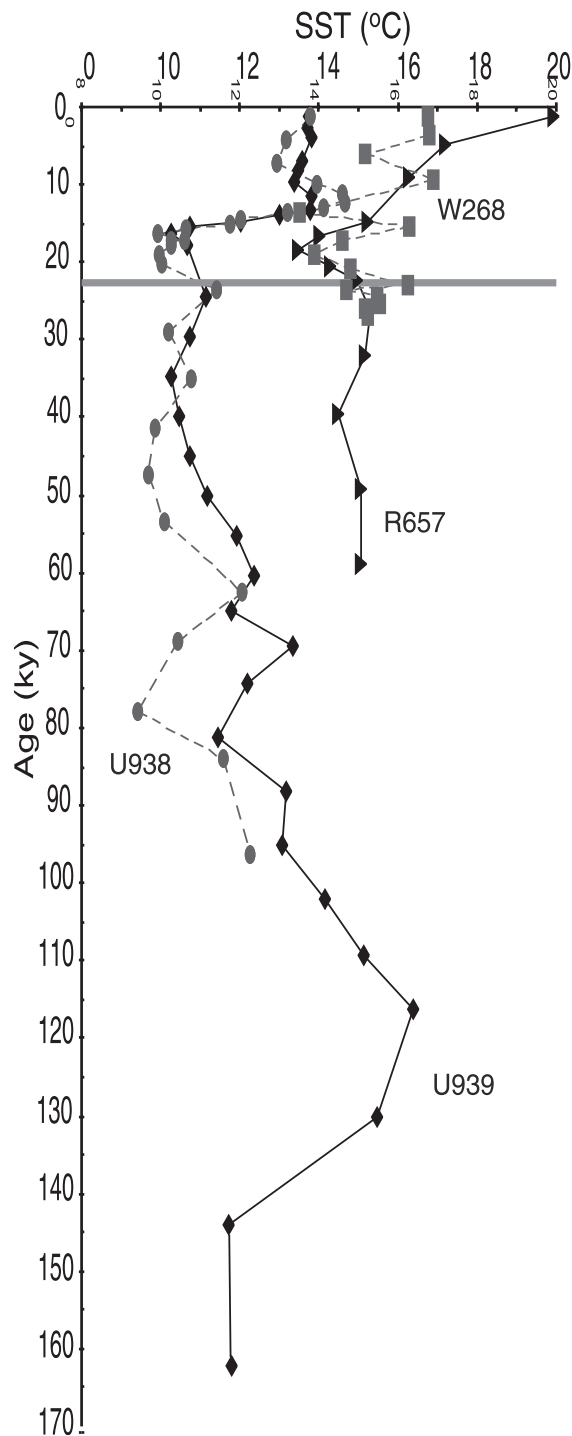


Figure 4. Alkenone-based temperature estimates reported against age. Solid triangles, subtropical core R657; solid circles, subtropical core W268; solid squares, subpolar core U938; solid diamonds, subpolar core U939. Summer temperatures in the last glacial maximum were 4°C cooler in both water masses, similar to winter conditions in the area today. The temperature gradient across the front remained ~4°C in both the Holocene and last glacial periods. In isotope stage 3 the gradient is slightly greater at ~6°C due to subpolar waters remaining as cool as during the glaciation while subtropical waters were intermediate between glacial and Holocene values. In isotope stage 5, subpolar summer temperatures were as warm as Holocene subtropical waters.

ous with little disturbance over the last few glacial cycles [Carter *et al.*, 2000].

[15] All pre-Holocene ^{14}C dates on bulk carbonate (two to four samples per core) appear to be too old by as much as several thousand years in comparison with the other stratigraphic parameters in the core (Table 2 and Figure 2). We ascribe this to reworked detrital carbon which, when present, has been shown to increase the apparent age of deglacial samples by as much as 2500 years [Jones *et al.*, 1989] because of different fractions of the carbon present in sediments varying by as much as 10,000 years [Eglinton *et al.*, 1997]. Therefore we have disregarded pre-Holocene bulk ^{14}C dates and rely on our other stratigraphic controls for oxygen isotope stages 2 and older. The ^{14}C dates were not converted to calendar ages in calculating depth to age conversions.

[16] Sedimentary carbonate content in this location shows the pattern typical of the Southern Ocean region [Carter *et al.*, 2000; Howard and Prell, 1994; Wright *et al.*, 1995] with higher carbonate contents during interglaciations and lower contents during glaciations. The changes in carbonate content and $\delta^{18}\text{O}$ are essentially synchronous in all cores at the isotopic stage 2.0 (12,050 year) boundary (Figure 2). Isotope stage boundaries 3.0 (24 ka), 4.0 (59 ka), 5.0 (74 ka), and 6.0 (130 ka) are less well defined than 2.0 and are assigned in all cores based on the best fit between variations in carbonate percentage and $\delta^{18}\text{O}$ according to Martinson *et al.* [1987]. Depth to age conversions are based on linear interpolation between assigned time points.

[17] Pre-Holocene AMS ^{14}C dates in core W268 (Table 2 and Figure 2d) are reversed. The sedimentation rate of ~1 cm kyr $^{-1}$ above the Kawakawa Tephra is low, and the location of the core closer to the crest of the Rise where sediments become affected by bottom currents [Barnes, 1992; Carter *et al.*, 2000] leads us to conclude that a combination of bioturbation [Boyle, 1984] and winnowing are the cause of the noisy deglacial signal in the core. The resulting poor resolution prevents the use of this core for detailed analysis of the glacial to interglacial transition. However, results from the full Holocene and glacial levels record consistent temperatures which can be assumed to be indicative of glacial and Holocene conditions and can be used for comparisons of these two climatic periods [Boyle, 1984].

3.2. Core Top and Modern Sea Surface Temperatures

[18] Alkenone-based $U_{37}^{K'}$ SST reconstructions were generated for all four cores (i.e., two from each side of the front). Cores R657 and W268 sit in subtropical waters today with the most northern core, R657, located beyond the frontal zone (Figure 1). Slightly south and west of R657, core W268 is located farther upslope and is seasonally in subtropical waters or within the subtropical front. The modern (Recent) temperature reconstruction from the core top in R657 is 19°C (Figure 3). Numerical data are available from the World Data Center for Paleoclimatology.¹ The $U_{37}^{K'}$ core top SST estimate of 17°C in core W268 reflects its more proximal location relative to the front. The average of 18.4°C for the two core top $U_{37}^{K'}$ SST values from north of the rise agrees well with the summer SST in subtropical waters in the area (Figures 3 and 4) [Chiswell, 1994; Garner, 1967; Gilmour and Cole, 1979]. South of the front, core U939 sits on the southern flank of the rise and the southern edge of the seasonal range of the STF, while core U938 sits farther south on the flat of the Bounty Trough well to the south of the STF. Both have core top reconstructions of ~14°C, which are equivalent to summer SST for subpolar waters in this location (Figure 3).

¹ Supporting data are available electronically from World Data Center-A for Paleoclimatology, NOAA/NGDC, 325 Broadway, Boulder, CO 80303, USA (email: paleo@ngdc.noaa.gov; URL: <http://www.ngdc.noaa.gov/paleo/paleo.html>).

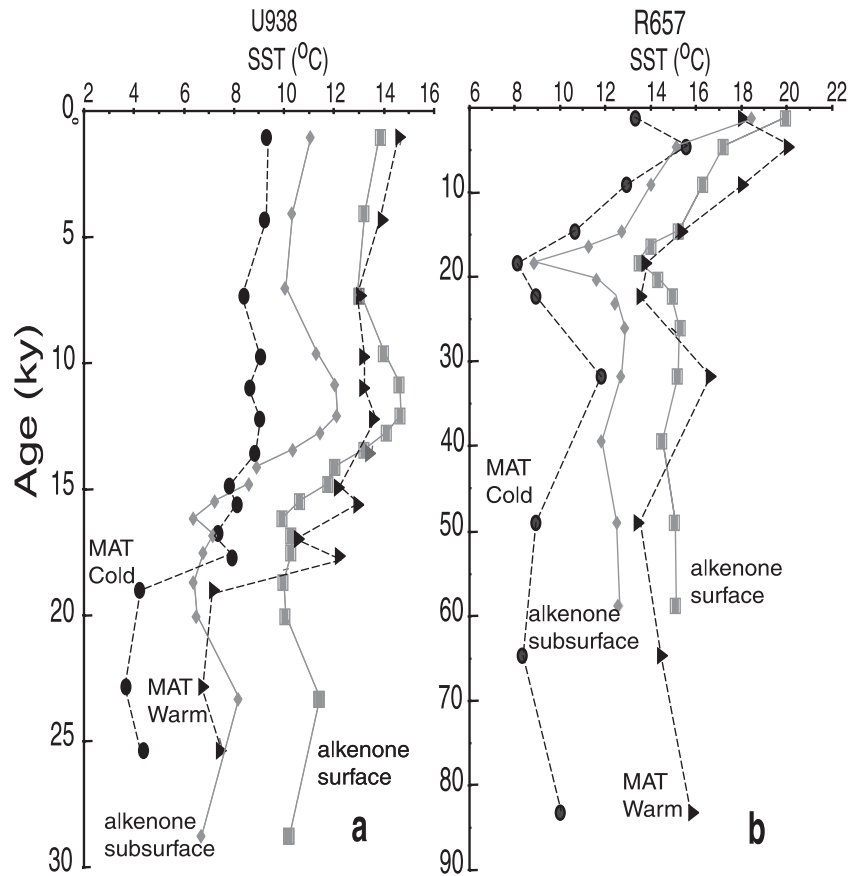


Figure 5. Foraminiferal-based temperature estimates: (a) subpolar core U938 and (b) subtropical core R657. Warm season foraminiferal assemblage MAT temperature estimates are shown by triangles and dotted line. Cool season MAT are shown by ovals and dotted line. Alkenone summer SST estimates based on *Sikes and Volkman* [1993] calibration are shown by squares and solid line. Alkenone SST estimates representing subsurface production using *Prahl et al.* [1988] calibration are shown by diamonds and solid line. MAT summer temperature estimates agree well with summer alkenone SST estimates in subtropical waters. MAT summer temperature estimates agree well with summer alkenone SST estimates in the subpolar waters in the Holocene but with subthermocline alkenone temperature estimates in the glacial maximum suggesting a change in controls on foraminiferal SST estimates in this water mass in the glaciation.

[19] Faunal SST reconstructions were generated for one core in each water mass (Figures 3 and 5). MAT summer core top SST for R657 is 18.1°C (winter SST reconstructions are 13.3°C; Figure 3b). This is 2°C cooler than the alkenone-derived estimates, equal to February Comprehensive Ocean-Atmosphere Data Set (COADS) (Figure 3), 1°–2°C cooler than Levitus summer averages [*Levitus, 1984; Levitus and Boyer, 1994*], and in agreement with February satellite-derived temperatures [*Chiswell, 1994*] for subtropical waters (Figures 6a and 6f). The two core averages for the subtropical U_{37}^K SST and the MAT differ by ~1°C but agree within the errors of the methods ($\pm 2^\circ\text{C}$ for both methods [*Sikes et al., 1997; Prell et al., 1999*]). For a within-technique comparison, there are available sediment trap derived MAT temperature estimates from this area [*King and Howard, 2001*]. *King and Howard* [2001] obtained a summer SST of 20°C, which agrees well with the alkenone-based core top estimate in core R657. In contrast, the MAT estimate from that core top (18°C) agrees better with the alkenone-derived estimate from core W268 (17°C), a plausible situation, given the closeness of the cores to the complex frontal location.

[20] Our southern cores are located farther from the main frontal area. The subpolar warm season core top MAT estimate

in U938 (Figure 3a) is 14.7°C (winter SST of 9.4°C; Figure 3b), which agrees within 0.5°C with the alkenone estimates. Here, in contrast to the situation north of the rise, temperature reconstructions from both techniques (Figures 3a and 6f) agree within 0.5°C and agree well with observational SST of ~14°C (for August, *COADS* [1999], *Chiswell* [1994], *Levitus* [1984], and *Levitus and Boyer* [1994]). All our core top SST estimates agree well with previous work on Holocene samples from this area [*Weaver et al., 1997*].

[21] These sediment core top temperatures largely reflect the modern temperature gradient across the front of ~4°C with each technique being internally consistent and in agreement with hydrological studies from the immediate area of the cores [*Chiswell, 1994; Garner, 1967; Gilmour and Cole, 1979*]. The alkenone-derived values suggest a greater temperature difference across the front of 4.7°C, in agreement with summer observational data, whereas the foraminiferal gradient of 3.4°C is more indicative of spring or fall conditions (Figure 6c) [*Chiswell, 1994*]. In contrast, modern MAT sediment trap-derived summer temperatures in Southern Ocean waters [*King and Howard, 2001*] are 2°C cooler than our core top reconstructions and the observational SSTs. The sediment trap summer SST reconstruction of ~12°C is midway

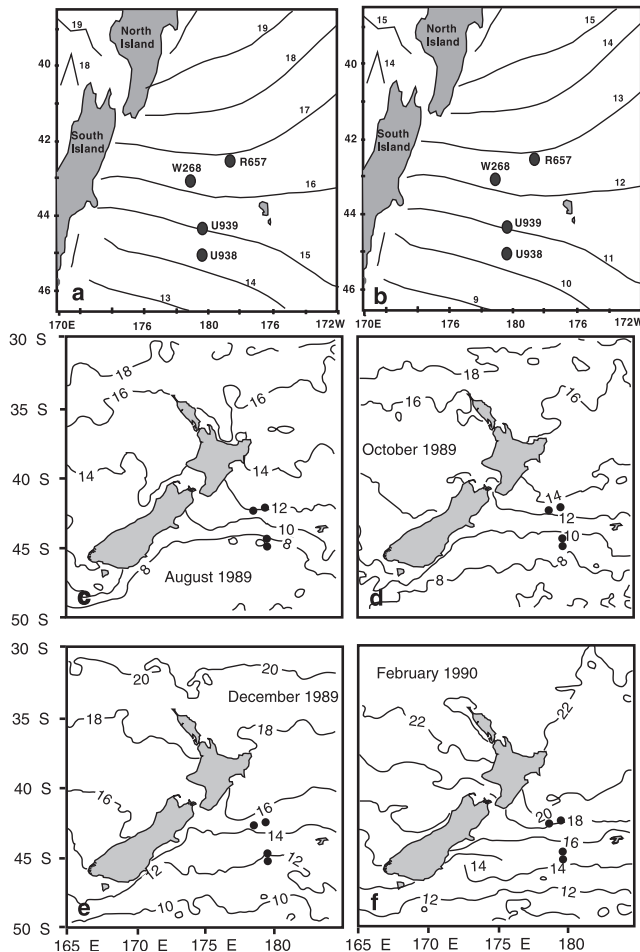


Figure 6. Modern sea surface temperatures east of New Zealand. Solid circles are the location of the cores used in this study. (a) Summer season temperatures from *Levitus* [1984] and *Levitus and Boyer* [1994]. (b) Winter season temperatures from *Levitus* [1984] and *Levitus and Boyer* [1994]. (c) Surface temperatures in the region for August 1989 taken from satellite-based advanced very high resolution radiometer (AVHRR) data [Chiswell, 1994]. (d) Satellite-based temperatures for October 1989. (e) Satellite-based temperatures for December 1989. (f) Satellite-based temperatures for February 1990. The *Levitus* and *COADS* database averages SST over several years but also over a 1° – 2° latitudinal footprint, averaging out the 4°C temperature gradient across the STF. The short-term data show both the pinching together of isotherms associated with the steep gradient of temperature across the front and variability in the position of the front through the year. Away from the front the satellite data reproduce the multiyear average temperatures of the *COADS* database.

between winter and summer SST in this location (Figure 3). Interestingly, the north to south trap reconstructions indicate an across-front SST difference of almost 9°C , which is greater than seen at any time of the year.

3.3. Down Core Temperature Reconstructions

[22] North of the Rise in core R657 the U_{37}^K -derived temperatures rise smoothly and continuously from the glacial low of 13.5°C to a core top high of 20.0°C (Figure 4). This is a glacial to interglacial

temperature change of 6.5°C . Glacial temperatures in core W268 are $\sim 14^{\circ}\text{C}$ and fluctuate widely in the transition before settling in the Holocene at $\sim 16.8^{\circ}\text{C}$, $\sim 3^{\circ}\text{C}$ warmer. The fluctuation may be due to bioturbation, but movements and variations in the front cannot be ruled out. In both cores, temperatures in isotope stage 3 are the same at $\sim 15^{\circ}\text{C}$, which is $\sim 1^{\circ}\text{C}$ warmer than at stage 2.

[23] Subpolar cores U938 and U939 have U_{37}^K glacial temperature lows of $\sim 10^{\circ}\text{C}$ that shift rapidly to Holocene temperatures of $\sim 13^{\circ}$ – 15°C . The early Holocene has the warmest postglacial temperatures of 14° – 15°C occurring at 11–12 ka (Figure 4). Mid-Holocene temperatures are $\sim 1^{\circ}\text{C}$ cooler than the core tops, with an extended plateau of $\sim 13.8^{\circ}\text{C}$ at 9–6 ka. In isotope stages 3 and 4 the temperatures remain much cooler than stage 1, $\sim 1^{\circ}$ – 2°C warmer than stage 2 (10° – 13°C). Core U939 has U_{37}^K reconstructions extending back to the last interglacial (stage 5) when temperatures exceeded 16°C and were as much as 2.5°C warmer than maximum Holocene temperatures.

[24] MAT warm season temperature reconstructions in core R657 show glacial temperatures of 13.6°C in isotope stage 2 rising slowly and gradually to a Holocene maximum at 4.5 ka (Figure 5b). Temperatures peak in the Holocene and drop by 2°C to 20.0°C between the early Holocene and the core top (4.5 ka). The subtropical glacial to interglacial temperature change was 4.5° – 6.5°C depending on the choice of core top estimate or the Holocene maximum temperature. In subpolar waters (core U938), warm season SSTs have a low of 6.8°C in the glaciation. SST reconstructions exhibit a similar early Holocene maximum (of 13.8°C) seen in the U_{37}^K record for this core, but Holocene warmest temperatures are at the core top (14.7°C). Glacial to interglacial temperature change is 6° – 8°C depending on the choice of core top maximum or the Holocene average as a benchmark. Winter SST reconstructions essentially parallel the warm season temperatures but are 4°C cooler (Figure 5a).

[25] In the last glaciation, U_{37}^K temperature estimates are on average 4.7°C cooler in subtropical waters and an average of 3.6°C cooler in subpolar waters. Foraminiferal reconstructions indicate a glacial-interglacial temperature change of $\sim 5^{\circ}\text{C}$ in subtropical waters in agreement with the alkenone-based estimates and $\sim 7^{\circ}\text{C}$ cooling in subpolar waters, which is about twice that of the U_{37}^K reconstructions.

4. Discussion

4.1. Core Top Temperature Reconstructions: Differences Among Data Sets

[26] Our subpolar SST estimates agree well with the *COADS* SST at 45°S , whereas our temperature estimates for subtropical waters north of the rise appear to be as much as 2.5°C too warm [*COADS*, 1999] (Figures 3 and 6a). Frontal zones such as the STF are locations of steep temperature gradients for which it is difficult to get accurate temperature estimates from world data bases that average many years of data [*COADS*, 1999; *Levitus*, 1984; *Levitus and Boyer*, 1994], as do core tops. World data bases are usually preferable for paleoceanographic reconstructions; however, the data in these are averaged over a 1° – 2° latitude footprint, providing only four data points across our study area, smoothing away the characteristic steep gradient of the front (Figures 3, 6a and 6b). High-resolution short-term studies, although lacking the advantage of multiyear averaging, provide more realistic across-front temperature profiles [e.g., *Belkin and Gordon*, 1996; *Chiswell*, 1994; *Garner*, 1967; *Gilmour and Cole*, 1979; *Uddstrom and Oien*, 1999]. *Chiswell* [1994] presents monthly mean temperatures for 1989–1990 calculated from satellite images which agree well with the hydrocast data from summer 1963 and spring 1976 [*Garner*, 1967; *Gilmour and Cole*, 1979]. Comparison of data of *Chiswell*

[1994]; Levitus [1984]; Levitus and Boyer [1994]; and COADS [1999] indicates that Levitus data underestimate summer temperatures in the area of our northern cores by up to 2°C and tend to underestimate summer temperatures by up to 1°C at our southern sites (Figures 3 and 6).

[27] Observational temperatures from the midpoint of the frontal zone (43°S) agree with the *Chiswell* [1994] data set for summer and northern winter values. This observation of the midpoint agreement and seasonal discrepancies that are asymmetrical to the north and south is indicative of the seasonal north-south movement of the front observed by *Chiswell* [1994]. Although its location shifts continually, the front sits preferentially to the north of the rise in summer and to the south in winter (compare Figure 6c with Figure 6f) and is marked by ever-present mesoscale eddies [*Chiswell*, 1994; *Roemmich and Sutton*, 1998; *Uddstrom and Oien*, 1999]. Thus our southern cores may be interpreted as being located farther from the frontal area, particularly in summer, whereas the variation between estimates and observations to the north, in particular, the 3°C between core top U_{37}^K SST estimates, is an indication of the complexity of the temperature structure in this area.

[28] On the Chatham Rise the choice of U_{37}^K calibration affects the interpretation of the data, and considering alternate temperature reconstructions sheds insight on the interpretation of SST reconstructions on the Chatham Rise. The *Sikes and Volkman* [1993] U_{37}^K calibration provides realistic summer temperature reconstructions for this area that reproduce summer season SSTs of ~14°C to the south and ~16°–18°C to the north which are directly comparable to foraminiferal estimates (Figures 3 and 6). In contrast, SSTs calculated using *Prahl et al.* [1988] (or any global estimate such as *Sikes et al.* [1997] or *Müller et al.* [1998]) reconstruct temperatures cooler than annual averages and represent winter temperatures particularly to the south of the rise (Figure 3b).

[29] Production at the base of the mixed layer (subsurface) is likely occurring on the Chatham Rise [*Bradford-Grieve et al.*, 1997]. Interpreting modern SST reconstructions based on *Prahl et al.* [1988] would suggest that much of the annual production occurs in late winter, whereas maximum phytoplankton production is known to occur in spring to summer, analogous to the situation in the North Pacific [*Prahl et al.*, 1993]. A more likely interpretation is near-surface production early in the season moving deeper in spring to summer or subsurface production throughout the growth season [*Prahl et al.*, 1993]. These temperature reconstructions produce an 8°C gradient across the front, twice that actually seen in any season today and similar to the 9°C indicated by MAT sediment trap-based reconstructions [*King and Howard*, 2001], suggesting the influence, at least intermittently, of subsurface conditions influencing foraminiferal temperature reconstructions in this area.

[30] Foraminiferal core top reconstructions on average agree better, in both water masses, with the *Sikes and Volkman* [1993] calibration in Holocene samples, for which we assume conditions similar to today. In addition to providing the most accurate warm season temperature estimates for the season of maximum bloom, using the *Sikes and Volkman* [1993] calibration gives an across front temperature gradient of 4°–5°C (Figure 3), reproducing the actual gradient seen across the front quite well (Figure 6). These considerations suggest the use of this calibration thus gives a better framework against which to compare down core SST reconstructions.

4.2. Last Glacial Temperature Reconstructions Across the Front

[31] Alkenone-derived SST estimates for the last glaciation indicate that the extent of cooling both north and south of the

front was similar (i.e., 3°–6°C in the north and 4°C in the south) with summer temperatures of ~14°C in subtropical waters and 12°C in subpolar waters, which are, coincidentally, the same SSTs as winter in this region today. This temperature profile reconstructs an average glacial cross-frontal temperature gradient of 4.7°C, slightly larger than in the Holocene, due to a greater cooling of subtropical waters (data from core R657) than subpolar waters (Figure 4). MAT estimates show the same 4°C drop in subtropical waters as estimates from the alkenones. In contrast, the MAT estimates for subpolar waters, although similar to other faunal reconstructions for this location [*Weaver et al.*, 1997; *Wells and Okada*, 1997], show twice the cooling (~8°C) indicated by the alkenones. The agreement of our MAT reconstructions with previously published transfer function SST estimates [*Barrows et al.*, 2000; *Weaver et al.*, 1997] suggests that it is not a function of how the values are calculated but indicates that there might be more fundamental factors specific to the faunal technique that lead to inaccurate SST reconstructions for the last glaciation as suggested by *Wells and Okada* [1997]. Notwithstanding these differences in absolute temperatures returned by the different techniques, both reconstructions show that a strong temperature gradient remained across the rise, indicating that the front did not move off the Chatham Rise at the Last Glacial Maximum, in agreement with other studies [*Barrows et al.*, 2000; *Fenner et al.*, 1992; *Nelson et al.*, 1993; *Weaver et al.*, 1997].

[32] A doubling of the SST gradient across the STF in the last glaciation is somewhat difficult to explain. Arguably, there could be some sort of chilling effect caused by the proximity of the mountainous subcontinent of New Zealand and increased current velocities [*Nelson et al.*, 2000]. However, more extreme cooling of subpolar waters relative to subtropical waters east of New Zealand is not supported by terrestrial temperature reconstructions in NZ which show an even temperature drop of ~4°–5°C across both islands, with no record of an enhanced temperature drop for the South Island [*Pillans et al.*, 1993]. Nor is it supported by studies which indicate enhanced cooling of coastal subtropical waters [*Nelson et al.*, 2000] which would diminish the across-front temperature difference. Elsewhere in the Southern Ocean, paleoreconstructions, many based on foraminiferal assemblages [e.g., *Barrows et al.*, 2000; *Howard and Prell*, 1992], indicate the maintenance of the ~4°C gradient across the front, an ocean-wide subtropical to subpolar surface water cooling of around 4°C [*Barrows et al.*, 2000; *Howard*, 1992; *Wells and Okada*, 1996; *Wells and Chivas*, 1994; *Wells and Okada*, 1997], and movement of isotherms to the north by 3°–5° latitude [*Howard and Prell*, 1992; *Morley*, 1989]. A cooling of 8°C on the Chatham Rise would require a movement north of isotherms by 15° of latitude south of the STF only in the New Zealand area, and greater cooling than the adjacent landmass, both patterns which are not seen anywhere else in the region [*Barrows et al.*, 2000].

[33] The agreement of our temperature reconstructions in both water masses in the Holocene and their divergence in glacial subpolar waters suggest that there are physical or biological reasons for the differences. Physical changes causing this difference in response could be associated with higher wind stresses during the glaciation [*Stewart and Neall*, 1984] enhancing upwelling and placing the subsurface thermocline in proximity to the productivity maximum. Foraminifera, living deeper than phytoplankton, would effectively be within the thermocline thereby recording cooler temperatures. Additionally, an enhanced difference in seasonality, with more distinction in growth seasons between alkenone producers and foraminifera, could contribute to differences between the techniques not seen in the modern reconstructions. Today, the faunal assemblages in this

area have a high proportion of *Globorotalia inflata* [Weaver *et al.*, 1997]. *G. inflata*, the indicator species for the transitional assemblage, is the only foraminifera associated with the upwelling assemblage [Molfini *et al.*, 1982] expected to be abundant in the cool conditions at the STF today. Sediment trap reconstructions [King and Howard, 2001] return SSTs closer to spring than summer temperatures, suggesting a strong association with spring conditions. Increased winds and upwelling associated with the front may have caused the fauna to become skewed to those associated with spring and upwelling conditions, while the alkenone producers may have remained associated with summer and more stratified conditions. The probability that a shift in foraminiferal seasonality occurred in this area is further supported by isotopic results indicating that *Globigerina bulloides* growing in subtropical waters shifted their season of growth from winter to summer during the glaciation [Nelson *et al.*, 2000].

[34] The doubling of the SST gradient across the front and the extremely cool temperatures seen only in subpolar waters are internally consistent within the foraminiferal techniques [Barrows *et al.*, 2000; Weaver *et al.*, 1997]. The discussion above concerning the choice of alkenone calibrations producing either a 4°C or an 8°C gradient for the Holocene reconstructions across the front and sediment trap MAT reconstructions of a 9°C gradient for one modern summer season provides a model for how a more prevalent subsurface habitat could skew glacial SST reconstructions. The Prahl *et al.* [1988] calibration, which might be considered a subsurface alkenone calibration for this area, agrees with glacial age winter MAT SST estimates in subtropical waters as it does in the core tops but with summer MAT SST estimates for glacial subpolar waters. This supports the suggestion that a change in habitat for subpolar species of foraminifera at the Last Glacial Maximum may have skewed foraminiferal analog results. The modern analog for glacial foraminiferal assemblages is at the present-day Antarctic polar frontal zone, presently 8°–10° farther south than the STF. Previous work indicates that in the LGM the polar front was at 47° in this region [Weaver *et al.*, 1997]. The presence of the polar glacial foraminiferal assemblages well north of the glacial polar frontal zone and proximal to the STZ suggests biological enhancement of the polar aspect of those faunas, either a deeper habitat and/or the annual bloom season occurring earlier in subpolar waters than today. This would cause the glacial foraminifera to record cooler temperatures in subpolar waters and exhibit the observed enhanced temperature gradient across the front. Such a situation could be hard to detect within the foraminiferal assemblage because of the low species diversity in subantarctic waters.

[35] Similarly, the alkenone producers may have shifted their season of production to the very short, warmest interval of the summer or to a shallower level in the glaciation. Thus they may not have captured the full range of glacial-interglacial SST change, whereas the foraminifera may have reflected production over more of the (6°–8°C cooler) average year. Such a shift in seasonality would, however, have required these algae to be restricted from growing in temperatures that they commonly exist in today.

[36] Importantly, these proposed shifts in the seasonal production and depth habitat of the foraminifera and haptophytes may have occurred in either or both organisms in the last glaciation. The implication of such changes, in any combination, implies similar conditions in the surface water physical parameters in subpolar waters south of the Chatham Rise in the last glaciation. That is, despite deep mixing associated with increased windiness in the winter [Stewart and Neall, 1984], in summer, there was a shallower mixed layer, enhanced stratification, and a warm (relatively warmer) surface layer in summer subpolar water. These results

support those of Francois *et al.* [1997] suggesting enhanced seasonal stratification of subantarctic waters in the glaciation.

4.3. Down Core Temperature Reconstructions Across the Front

[37] The late deglacial to early Holocene temperatures recorded in the subpolar cores show an extended plateau with earliest Holocene temperatures (11–12 kyr ago) of 14°–15°C being the warmest temperatures seen in both foraminiferal and alkenone reconstructions. These SSTs are comparable to modern values and predate a 1°–2°C cooling that occurred in the mid-Holocene (8–4 ka) (Figure 4). This early Holocene temperature maximum appears to be regionally widespread in Southern Hemisphere temperature records from the Indian Ocean, Australian, and New Zealand regions of the Southern Ocean [Ikehara *et al.*, 1997; Weaver *et al.*, 1998; Wells and Okada, 1996, 1997]. It is also seen in STF and subtropical waters in the southern Indian Ocean [Hutson, 1980; Labeyrie *et al.*, 1996; Morley, 1989]. In contrast, this plateau is absent from our subtropical cores except for one point in the foraminifera-derived SST plot in core R657, although it may have been missed simply because of the low resolution of the record in these cores.

[38] Subtropical temperature reconstructions in marine isotope stage 3 are 2°C cooler than in the Holocene and 2°C warmer than the glacial SSTs. In contrast, subpolar stage 3 SST reconstructions remain similar to glacial temperatures for both techniques. For periods earlier than stage 3, only U_{37}^K temperature reconstructions are available for both water masses which show a temperature gradient of 6°C, slightly greater than in the glacial and Holocene. This suggests that during stage 3, subpolar conditions were cooler or more severe relative to subtropical conditions.

[39] Alkenone temperature reconstructions extend to the last interglacial (stage 5) for only the subpolar core U939, and alkenone-based temperature estimates for subtropical waters are unavailable for stage 5. SSTs of 16°C indicate that stage 5 was warmer than the Holocene by as much as 3°C, with temperatures comparable to those seen in Holocene subtropical waters. A warmer than Holocene stage 5 is seen regionally in the southern Indian Ocean [Howard and Prell, 1992; Labeyrie *et al.*, 1996; Morley, 1989], south of Tasmania [Ikehara *et al.*, 1997], in STF waters off Western Australia [Wells and Wells, 1995], and locally at Ocean Drilling Program (ODP) Site 594 [Wells and Okada, 1997]. However, faunal reconstructions from the south side of the Chatham Rise [Weaver *et al.*, 1998] across stage 5 show SSTs ~3°C cooler than in the Holocene and equivalent to stage 3. Subtropical stage 3 reconstructions from that study are equal to both our and their Holocene values of 18°C [Weaver *et al.*, 1998]. The Weaver *et al.* [1998] reconstructions indicate a gradient across the front as enhanced at stage 5 as at stage 2. A comparison of their subtropical faunal estimates and our alkenone subpolar reconstructions indicate (as in stages 1 and 2) that the frontal gradient was the same as today or slightly reduced in stage 5. This is consistent with other studies elsewhere in the region [Howard and Prell, 1992; Labeyrie *et al.*, 1996; Morley, 1989], suggesting that as in the last glaciation, faunal subpolar reconstructions in stage 5 may have the same cool bias as the glacial faunal estimates discussed above.

[40] Alternatively, warm U_{37}^K SST estimates could be due to a change in species composition of alkenone producers in isotope stage 5. *Emiliania huxleyi* did not achieve dominance in the Southern Ocean haptophyte flora until after 85 ka [Thierstein *et al.*, 1977]. *Gephyrocapsa oceanica* is likely to have been the predominant producer of alkenones at that time, and there is evidence that a predominance of *G. oceanica* [Sawada *et al.*, 1996; Volkman *et al.*, 1995] would return warmer estimates for the same U_{37}^K values. However, there is debate whether differences in

alkenone distributions between *E. huxleyi* and *G. oceanica* could lead to different temperature responses with evidence suggesting that any differences in alkenone distributions in the two species fall within the intraspecific variability [Conte *et al.*, 1998]. In the Chatham Rise sediments, alkenones could provide robust temperature estimates for this time period even though species compositions would have changed.

5. Conclusions

[41] During the deglaciation and the Holocene, SST reconstructions based on alkenones and foraminiferal assemblages agree with one another and appear to provide realistic temperature reconstructions across the subtropical front region on the Chatham Rise area. In contrast, these two proxies give differing estimates of glacial and earlier SSTs. Climate-induced changes within the frontal region or mesoscale movements of the subtropical front have the potential to alter the surface water structure and the biology of the area. This may lead to disagreement between temperature estimates based on the foraminiferal modern analog technique and U_{37}^K index at times in the past.

[42] Specific conclusions are as follows.

1. SST estimates for the Holocene using both techniques are similar to modern values. Subpolar waters exhibit an early Holocene temperature maximum that is 1°–2°C warmer than the late Holocene, a phenomenon that is widespread throughout the region.

2. Alkenone reconstructions for isotope stage 3 show temperatures intermediate between the glaciation and modern values. Subtropical water temperatures were slightly cooler than during the Holocene (15°C), and subpolar waters were close to glacial temperatures causing the across-front gradient to be slightly greater at that time (~6°C).

3. Alkenone reconstructions indicate subpolar waters were >2°C warmer than modern subpolar waters during isotope stage 5. Comparison to foraminiferal reconstructions [Weaver *et al.*, 1998] suggests a smaller temperature gradient across the front at that time, which is also seen elsewhere in the region.

4. In the last glaciation both temperature proxies indicate that subtropical waters were ~4°C cooler than today, with glacial summer temperatures similar to winter temperatures today.

5. In subpolar waters in the last glaciation the alkenone index indicates a ~4°C cooling, the same magnitude of cooling seen in subtropical waters. Summer temperatures were the same as modern and Holocene winter values, and the glacial temperature gradient across the front was the same as modern (~4°C). In contrast, foraminiferal assemblages show an 8°C cooling in the glaciation, twice that seen in U_{37}^K estimates and subtropical waters and thus indicate a doubling of the temperature gradient across the front. Glacial alkenone temperature reconstructions are in better agreement with the majority of Southern Ocean subpolar reconstructions and terrestrial temperature estimates from the New Zealand landmass. The difference between these biologically based SST reconstructions may have been due to a change in seasonality and timing of respective blooms across the front resulting in relatively cooler estimates from the foraminifera compared to the alkenones. Regardless of the specific reason, the differences between the techniques suggest that there were climatically related changes in surface water properties in subpolar waters and the STF, such as seasonal upwelling associated with increased winds during the glaciation and/or increased stratification of the surface layer.

6. Our results support previous work indicating that the STF remained fixed over the Chatham Rise during the Last Glacial Maximum.

[43] **Acknowledgments.** Special thanks go to Scott Nodder and members of the New Zealand National Institute for Water and Atmospheric Research's seagoing group for generous ship time and assistance under difficult conditions in order to obtain the cores used in this study. We thank Tom Guilderson who assisted with AMS dates to improve the stratigraphy in the cores. Thanks also go to Naomi Parker and Cecelia Abbott who wrangled cores and forams for the study. A special appreciation is owed to Lisette Robertson for her tireless and cheerful assistance in data production and management and especially for her skill in drafting the maps. Lionel Carter, Toni Rosell-Melé, and Phil Weaver provided reviews which helped improve the manuscript.

References

- Anderson, D. M., W. L. Prell, and N. J. Barratt, Estimates of sea surface temperature in the Coral Sea at the Last Glacial Maximum, *Paleoceanography*, 4, 615–627, 1989.
- Barnes, P. M., Mid-bathyal current scours and sediment drifts adjacent to the Hikurangi deep-sea turbidite channel, eastern New Zealand: Evidence from echo-character mapping, *Mar. Geol.*, 106, 169–187, 1992.
- Barrows, T. T., S. Juggins, P. Dedecker, J. Theide, and J. I. Martinez, Sea surface temperatures of the southwest Pacific Ocean during the Last Glacial Maximum, *Paleoceanography*, 15, 95–109, 2000.
- Bé, A. W. H., and J.-C. Duplessy, Subtropical Convergence fluctuations and Quaternary climates in the middle latitudes of the Indian Ocean, *Science*, 194, 419–422, 1976.
- Belkin, I. M., and A. L. Gordon, Southern Ocean fronts from the Greenwich meridian to Tasmania, *J. Geophys. Res.*, 101, 3675–3696, 1996.
- Bottomley, M., C. K. Folland, J. Hsiung, R. E. Newell, and D. E. Parker, Global ocean surface temperature atlas "GOSTA", Meteorol. Off., Bracknell, UK, 1990.
- Boyle, E. A., Sampling statistic limitations on benthic foraminifera chemical and isotopic data, *Mar. Geol.*, 58, 213–224, 1984.
- Bradford-Grieve, J. M., F. H. Chang, M. Gall, S. Pickmere, and F. Richards, Size-fractionated phytoplankton standing stocks and primary production during austral winter and spring 1993 in the Subtropical Convergence region near New Zealand, *N. Z. J. Mar. Freshwater Res.*, 31, 210–224, 1997.
- Bradford-Grieve, J. M., P. W. Boyd, F. H. Chang, S. Chiswell, M. Hadfield, J. A. Hall, M. R. James, S. D. Nodder, and E. A. Shushkina, Pelagic ecosystem structure and functioning in the subtropical front region east of New Zealand in austral winter and spring 1993, *J. Plankton Research*, 21, 405–428, 1999.
- Butler, E. C. V., J. A. Butt, E. J. Lindstrom, and P. C. Tildesley, Oceanography of the Subtropical Convergence Zone around southern New Zealand, *N. Z. J. Mar. Freshwater Res.*, 26, 131–154, 1992.
- Carter, L., C. S. Nelson, H. L. Neil, and P. C. Froggat, Correlation, dispersal, and preservation of the Kawakawa Tephra and other late Quaternary tephra layers in the southwest Pacific Ocean, *N. Z. J. Geol. Geophys.*, 38, 29–46, 1995.
- Carter, L., H. L. Neil, and I. N. M. Cave, Glacial to interglacial changes in non-carbonate and carbonate accumulation in the SW Pacific Ocean, New Zealand, *Palaeogeogr. Palaeoclimatol. Palaeoecol.*, 162, 333–356, 2000.
- Chapman, M. R., N. J. Shackleton, M. Zhao, and G. Eglinton, Faunal and alkenone reconstructions of subtropical North Atlantic surface hydrography and paleotemperatures over the last 28 kyr, *Paleoceanography*, 11, 343–357, 1996.
- Chiswell, S. M., Variability in sea surface temperature around New Zealand from AVHRR images, *N. Z. J. Mar. Freshwater Res.*, 28, 179–192, 1994.
- Climate: Long-Range investigation, Mapping, and Prediction (CLIMAP), The surface of the ice-age earth, *Science*, 191, 1131–1137, 1976.
- Climate: Long-Range investigation, Mapping, and Prediction (CLIMAP), Seasonal reconstructions of the Earth's surface at the Last Glacial Maximum, *Geol. Soc. Am. Map Chart Ser.*, MC-36, 1981.
- Comiso, J. C., C. R. McClain, C. W. Sullivan, J. P. Ryan, and C. L. Leonard, Coastal zone color scanner pigment concentrations in the Southern Ocean and relationships to geophysical surface features, *J. Geophys. Res.*, 98, 2419–2451, 1993.
- Comprehensive Ocean-Atmosphere Data Set (COADS), World Ocean Atlas Seasonal Temperature Means, Pac. Mar. Environ. Lab., NOAA, Seattle, Wash., 1999.
- Conte, M. H., A. Thompson, D. Lesley, and R. P. Harris, Genetic and physiological influences on the alkenone/alkenoate versus growth temperature relationship in *Emiliania huxleyi* and

- Gephyrocapsa oceanica*, *Geochim. Cosmochim. Acta*, 62, 51–68, 1998.
- Edwards, R. J., and W. J. Emery, Australasian Southern Ocean frontal structure during summer 1976–77, *Aust. J. Mar. Freshwater Res.*, 33, 3–22, 1982.
- Eglinton, T. I., B. Benitez-Nelson, A. Pearson, A. P. McNichol, J. E. Bauer, and E. R. M. Druffel, Variability in radiocarbon ages of individual organic compounds from marine sediments, *Science*, 277, 778–796, 1997.
- Fenner, J., L. Carter, and R. Stewart, Late Quaternary paleoclimatic and paleoceanographic change over Chatham Rise, New Zealand, *Mar. Geol.*, 108, 383–404, 1992.
- Francois, R., M. A. Altabet, E. F. Yu, D. M. Sigman, M. P. Bacon, M. Frank, G. Bohrmann, G. Bareille, and L. D. Labeyrie, Contribution of Southern Ocean surface-water stratification to low atmospheric CO₂ concentrations during the last glacial period, *Nature*, 389, 929–935, 1997.
- Froggatt, P. C., and D. J. Lowe, A review of late Quaternary silicic and some other tephra formations from New Zealand: Their stratigraphy, nomenclature, distribution, volume, and age, *N. Z. J. Geol. Geophys.*, 33, 89–109, 1990.
- Garner, D. M., Hydrology of the southern Hikurangi Trench region, 36 pp., Natl. Inst. of Water and Atmos. Res., Lower Hutt, New Zealand, 1967.
- Gilmour, A. E., and A. G. Cole, The Subtropical Convergence east of New Zealand, *N. Z. J. Mar. Freshwater Res.*, 13, 553–557, 1979.
- Heath, R. A., The oceanic fronts around southern New Zealand, *Deep Sea Res., Part A*, 28, 547–560, 1981.
- Heath, R. A., A review of the physical oceanography of the seas around New Zealand, 1982, *N. Z. J. Mar. Freshwater Res.*, 19, 79–124, 1985.
- Howard, W. R., Late Quaternary paleoceanography of the Southern Ocean, Ph.D. thesis, Brown Univ., Providence, R. I., 1992.
- Howard, W. R., and W. L. Prell, Late Quaternary surface circulation of the southern Indian Ocean and its relationship to orbital variations, *Paleoceanography*, 7, 79–118, 1992.
- Howard, W. R., and W. L. Prell, Late Quaternary carbonate production and preservation in the Southern Ocean: Implications for oceanic and atmospheric carbon cycling, *Paleoceanography*, 9, 453–482, 1994.
- Hutson, W. H., The Agulhas Current during the late Pleistocene: Analysis of modern faunal analogs, *Science*, 207, 64–66, 1980.
- Ikehara, M., K. Kawamura, N. Ohkouchi, K. Kimoto, M. Murayama, T. Nakamura, T. Oba, and A. Taira, Alkenone sea surface temperature in the Southern Ocean for the last two deglaciations, *Geophys. Res. Lett.*, 24, 679–682, 1997.
- Jones, G. A., and P. Kateiris, A vacuum-gasometric technique for rapid and precise analysis of calcium carbonate in sediments and soils, *J. Sediment. Petrol.*, 53, 655–659, 1983.
- Jones, G. A., A. J. T. Jull, T. W. Linick, and D. J. Donahue, Radiocarbon dating of deep sea sediments: A comparison of accelerator mass spectrometer and beta-decay methods, *Radiocarbon*, 31, 105–116, 1989.
- King, A. L., and W. R. Howard, Seasonality of foraminiferal flux in sediment traps at Chatham Rise, SW Pacific: Implications for paleotemperature estimates, *Deep Sea Res., Part I*, 48, 1687–1708, 2001.
- Kipp, N. G., New transfer function for estimating past sea-surface conditions from sea-bed distribution of planktonic foraminiferal assemblages in the North Atlantic, in *Investigation of Late Quaternary Paleoceanography and Paleoclimatology*, edited by R. M. Cline and J. D. Hays, pp. 3–42, Geol. Soc. of Am., Boulder, Colo., 1976.
- Labeyrie, L. D., et al., Hydrographic changes of the Southern Ocean (southeast Indian sector) over the last 230 kyr, *Paleoceanography*, 11, 57–76, 1996.
- Levitus, S., Annual cycle of temperature and heat storage in the world ocean, *J. Phys. Oceanogr.*, 14, 727–746, 1984.
- Levitus, S., and T. Boyer, *World Ocean Atlas 1994*, vol. 2, *Oxygen*, NOAA Atlas NESDIS 2, 202 pp., Natl. Oceanic and Atmos. Admin., 1994.
- Martinson, D. G., N. G. Pisias, J. D. Hays, J. Imbrie, T. C. Moore, and N. J. Shackleton, Age dating and the orbital theory of the ice ages: Development of a high-resolution 0 to 300,000-year chronostratigraphy, *Quat. Res.*, 27, 1–30, 1987.
- Molfini, B., N. G. Kipp, and J. J. Morley, Comparison of foraminiferal, coccolithophorid, and radiolarian paleotemperature equations: Assemblage coherency and estimate concordancy, *Quat. Res.*, 17, 279–313, 1982.
- Morley, J. J., Variations in high-latitude oceanographic fronts in the southern Indian Ocean: An estimation based on faunal changes, *Paleoceanography*, 4, 547–554, 1989.
- Müller, P. J., G. Kirst, G. Ruhland, I. V. Storch, and A. Rosell-Melé, Calibration of the alkenone paleotemperature index U_{37}^K based on coretops from the eastern South Atlantic and the global ocean (60°N–60°S), *Geochim. Cosmochim. Acta*, 62, 1757–1772, 1998.
- Neil, H. L., Late Quaternary variability of surface and deep water masses—Chatham Rise, SW Pacific, Ph.D. thesis, Univ. of Waikato, Hamilton, New Zealand, 1997.
- Nelson, C. S., P. S. Cooke, C. H. Hendy, and A. M. Cuthbertson, Oceanographic and climatic changes over the past 160,000 years at Deep-Sea Drilling Project Site 594 off southeastern New Zealand, southwest Pacific Ocean, *Paleoceanography*, 8, 435–458, 1993.
- Nelson, C. S., I. L. Hendy, H. L. Neil, C. H. Hendy, and P. P. E. Weaver, Last glacial jetting of cold waters through the Subtropical Convergence zone in the southwest Pacific off eastern New Zealand, and some geological implications, *Palaeogeogr. Palaeoclimatol. Palaeoecol.*, 156, 103–121, 2000.
- Nodder, S. D., and L. C. Northcote, Episodic particulate fluxes at southern temperate mid-latitudes (42–45°S) in the Subtropical Front region, east of New Zealand, *Deep Sea Res., Part I*, 48, 833–864, 2001.
- Overpeck, J. T., I. C. Prentice, and T. Webb, Quantitative interpretation of fossil pollen spectra: Dissimilarity coefficients and the method of modern analogs, *Quat. Res.*, 23, 87–108, 1985.
- Pillans, B., M. McGlone, A. Palmer, D. Mildenhall, B. Alloway, and G. Berger, The Last Glacial Maximum in central and southern North Island, New Zealand: A paleoenvironmental reconstruction using the Kawakawa Tephra Formation as a chronostratigraphic marker, *Palaeogeogr. Palaeoclimatol. Palaeoecol.*, 101, 283–304, 1993.
- Prahl, F. G., L. A. Muehlhausen, and D. L. Zahnle, Further evaluation of long-chain alkenones as indicators of paleoceanographic conditions, *Geochim. Cosmochim. Acta*, 52, 2303–2310, 1988.
- Prahl, F. G., R. B. Collier, J. Dymond, M. Lyle, and M. A. Sparrow, A biomarker perspective on pyrrnnesiophyte productivity in the northeast Pacific Ocean, *Deep Sea Res.*, 40, 2061–2076, 1993.
- Prahl, F., T. D. Herbert, S. Brassell, N. Ohkouchi, M. Pagani, A. Rosell-Melé, D. Repeta, and E. Sikes, 2000. Status of alkenone paleothermometer calibration: Report from Working Group 3, *Geochem. Geophys. Geosyst.*, vol. 1, Paper number 2000GC000058 [4880 words, 7 figures]. Published November 7, 2000.
- Prell, W. L., The stability of low-latitude sea-surface temperatures: An evaluation of the CLIMAP reconstruction with emphasis on the positive SST anomalies, *Rep. 025*, U.S. Dep. of Energy, Washington, D. C., 1985.
- Prell, W., A. Martin, J. Cullen, and M. Trend, The Brown University Foraminiferal Data Base, *IGBP PAGES/World Data Center-A for Paleoclimatol. Data Contrib. Ser. 1999-027*, NOAA/NGDC Paleoclimatology Program, Boulder, Colo., 1999.
- Rintoul, S. R., J. R. Donguy, and D. H. Roemmich, Seasonal evolution of upper ocean thermal structure between Tasmania and Antarctica., *Deep Sea Res., Part I*, 44, 1185–1202, 1997.
- Roemmich, D., and P. Sutton, The mean and variability of ocean circulation past northern New Zealand: Determining the representatives of hydrographic climatologies, *J. Geophys. Res.*, 103, 13,041–13,054, 1998.
- Sawada, K., N. Handa, Y. Shiraiwa, A. Danbara, and S. Montani, Long chain alkenones and alkyl alkenoates in the coastal and pelagic sediments of the northwest North Pacific, with special references to the reconstruction of *Emiliania huxleyi* and *Gephyrocapsa oceanica* ratios, *Org. Geochem.*, 24, 751–764, 1996.
- Sikes, E. L., and L. D. Keigwin, Equatorial Atlantic sea surface temperatures for the last 30kyr: A comparison of U_{37}^K , $\delta^{18}O$, and foraminiferal assemblage temperature estimates, *Paleoceanography*, 9, 31–45, 1994.
- Sikes, E. L., and L. D. Keigwin, A reexamination of northeast Atlantic sea surface temperature and salinity over the last 16 kyr, *Paleoceanography*, 11, 327–342, 1996.
- Sikes, E. L., and J. K. Volkman, Calibration of alkenone unsaturation ratios (U_{37}^K) for paleotemperature estimation, *Geochim. Cosmochim. Acta*, 57, 1883–1889, 1993.
- Sikes, E. L., J. K. Volkman, L. G. Robertson, and J.-J. Pichon, Alkenones and alkenes in surface waters and sediments of the Southern Ocean: Implications for paleotemperature estimation in polar regions, *Geochim. Cosmochim. Acta*, 61, 1495–1505, 1997.
- Stewart, R. B., and V. E. Neall, Chronology of paleoclimatic change at the end of the last glaciation, *Nature*, 311, 47–48, 1984.
- Thierstein, H. R., K. R. Geitzenauer, B. Molfini, and N. J. Shackleton, Global synchronicity of Quaternary coccolith datum levels: Validation by oxygen isotopes, *Geology*, 5, 400–404, 1977.
- Uddstrom, M. J., and N. A. Oien, On the uses of high-resolution satellite data to describe the spatial and temporal variability of sea surface temperatures in the New Zealand region, *J. Geophys. Res.*, 104, 20,729–20,751, 1999.
- Volkman, J. K., Ecological and environmental factors affecting alkenone distributions in seawater and sediments, *Geochem. Geophys. Geo-*

- syst.*, vol. 1, Paper number 2000GC000061 [6314 words, 1 figure]. Published September 11, 2000.
- Volkman, J. K., S. M. Barrett, S. I. Blackburn, and E. L. Sikes, Alkenones in *Gephyrocapsa oceanica*: Implications for paleoclimatic studies, *Geochim. Cosmochim. Acta*, 59, 513–520, 1995.
- Weaver, P. P. E., H. L. Neil, and L. Carter, Sea surface temperature estimates from the Southwest Pacific based on planktonic foraminifera and oxygen isotopes, *Palaeogeogr. Palaeoclimatol. Palaeoecol.*, 131, 241–256, 1997.
- Weaver, P. P. E., L. Carter, and H. L. Neil, Response of surface water masses and circulation to late Quaternary climate change east of New Zealand, *Paleoceanography*, 13, 70–83, 1998.
- Wells, P. E., and A. R. Chivas, Quaternary foraminiferal bio- and isotope stratigraphy of ODP Holes 122-760A and 122-762B, Exmouth and Wombat Plateaus, northwest Australia, *Aust. J. Earth Sci.*, 41, 455–462, 1994.
- Wells, P. E., and R. Connell, Movement of hydrological fronts and widespread erosional events in the southwestern Tasman Sea during the late Quaternary, *Aust. J. Earth Sci.*, 44, 105–112, 1997.
- Wells, P., and H. Okada, Holocene and Pleistocene glacial palaeoceanography off southeastern Australia, based on foraminifera and nannofossils in hole V18-222, *Aust. J. Earth Sci.*, 43, 509–523, 1996.
- Wells, P. E., and H. Okada, Response of nannoplankton to major changes in sea-surface temperature and movements of hydrological fronts over DSDP Site 594 (south Chatham Rise, southeastern New Zealand), during the last 130 kyr, *Mar. Micropaleontol.*, 32, 341–363, 1997.
- Wells, P. E., and G. M. Wells, Large-scale reorganization of ocean currents offshore Western Australia during the late Quaternary, *Mar. Micropaleontol.*, 25, 289–291, 1995.
- Williams, D. F., Late Quaternary fluctuations of the Polar Front and Subtropical Convergence in the southeast Indian Ocean, *Mar. Micropaleontol.*, 1, 363–375, 1976.
- Wright, I. C., M. S. McGlone, C. S. Nelson, and B. J. Pillans, An integrated latest Quaternary (stage 3 to present) paleoclimatic and paleoceanographic record from offshore northern New Zealand, *Quat. Res.*, 44, 283–293, 1995.

W. R. Howard, Cooperative Research Centre for Antarctic and Southern Ocean Environment, GPO Box 252-80, Hobart, Tasmania 7001, Australia.

H. L. Neil, National Institute for Water and Atmosphere, Private Bag 14-901, Kilbirnie, Wellington, New Zealand.

E. L. Sikes, Institute of Marine and Coastal Sciences, Rutgers, State University of New Jersey, 71 Dudley Road, New Brunswick, NJ 80901-8521, USA. (sikes@imcs.rutgers.edu)

J. K. Volkman, CSIRO Marine Research, G.P.O. Box 1538, Hobart, Tasmania 7001, Australia.